Modeling hydrology and sediment transport in vegetative filter strips [☆]

Rafael Muñoz-Carpena[a], John E. Parsons[b,*], J. Wendell Gilliam[c]

[a]*Instituto Canario de Investigaciones Agrarias, Apdo 60 La Laguna, 38200Tenerife, Spain*
[b]*Department of Biological and Agricultural Engineering, North Carolina State University, Raleigh, NC 27695-7625, USA*
[c]*Soil Science, North Carolina State University, Raleigh, NC 27695-7625, USA*

Abstract

The performance of vegetative filter strips is governed by complex mechanisms. Models can help simulate the field conditions and predict the buffer effectiveness. A single event model for simulating the hydrology and sediment filtration in buffer strips is developed and field tested. Input parameters, sensitivity analysis, calibration and field testing of the model are presented. The model was developed by linking three submodels to describe the principal mechanisms found in natural buffers: a Petrov–Galerkin finite element kinematic wave overland flow submodel, a modified Green–Ampt infiltration submodel and the University of Kentucky sediment filtration model for grass areas. The new formulation effectively handles complex sets of inputs similar to those found in natural events. Major outputs of the model are water outflow and sediment trapping on the strip. The strength of the model is a good description of the hydrology within the filter area, which is essential for achieving good sediment outflow predictions or trapping efficiency. The sensitivity analysis indicates that the most sensitive parameters for the hydrology component are initial soil water content and vertical saturated hydraulic conductivity, and sediment characteristics (particle size, fall velocity and sediment density) and grass spacing for the sediment component. A set of 27 natural runoff events (rainfall amounts from 0.003 to 0.03 m) from a North Carolina Piedmont site was used to test the hydrology component, and a subset of nine events for the sediment component. Good predictions are obtained with the model if shallow uniform sheet flow (no channelization) occurs within the filter. © 1999 Elsevier Science B.V. All rights reserved.

Keywords: Surface runoff; Erosion modeling; Sediment; Vegetative filter strips

1. Introduction

Runoff carrying sediment from nonpoint sources

has long been recognized as a major pollutant of surface water. Sediment-bound pollutants, such as phosphorous and some pesticides are also a major pollution concern. Several management practices have been suggested to control runoff quantity and quality from disturbed areas. One such management practice is vegetative filter strips (VFS), which can be defined as (Dillaha et al., 1989) areas of vegetation designed to remove sediment and other pollutants from surface water runoff by filtration, deposition, infiltration, adsorption, absorption, decomposition,

and volatilization. These bands of planted or indigenous vegetation separate a water body from a land area that could act as a nonpoint pollution source. Vegetation at the downstream edge of disturbed areas may effectively reduce runoff volume and peak velocity primarily because of the filter's hydraulic roughness, and subsequent augmentation of infiltration. Decreasing flow volume and velocity translates into sediment deposition in the filter as a result of a decrease in transport capacity (Wilson, 1967). Barfield et al. (1979) and Dillaha et al., (1986) reported that grass filter strips have high sediment trapping efficiencies as long as the flow is shallow and uniform and the filter is not submerged.

As sediment is deposited from runoff in these vegetated zones, sediment-bound nutrients are also removed (Bolton et al., 1991; Flanagan et al., 1989). For nutrients attached to sediment (i.e. organic phosphorous, ammonium and organic N) the deposition process largely controls the effectiveness of the filter area, whereas infiltration is the controlling factor for soluble nutrients (such as nitrates and inorganic ortho-phosphates).

Several short-term studies have concentrated on evaluating the effectiveness of grass filter strips in trapping sediment and nutrients (Young et al., 1980; Daniels and Gilliam, 1989; Dillaha et al., 1989; Magette et al., 1989). They reported trapping efficiencies exceeding 50% for sediment and nutrients adsorbed to sediment, while dissolved nutrient trapping was not as efficient and sometimes an increase in nutrient losses has been reported (Dillaha et al., 1989; Magette et al., 1989).

Other areas that may be effective in improving off site surface water quality are riparian areas. They are defined (Lowrance et al., 1986; Mitsch and Goselink, 1986) as vegetated ecosystems along a water body through which energy, materials, and water pass. These areas encompass uplands, wetlands and combinations of both land forms. Cooper et al. (1987) estimated that as much as 90% of the sediment was deposited in the riparian area for a North Carolina watershed. Lowrance et al. (1986) concluded that riparian areas in Georgia were effective sinks for sediment.

Researchers (Dillaha et al., 1989; Parsons et al., 1991) have found that the filter length (L_t) controls sediment trapping up to an effective maximum length

value, thereafter, additional length does not improve filter performance. This maximum effective length depends on the source area, topography, and the hydraulic characteristics of the strip.

Several modeling efforts have been undertaken to simulate VFS efficiency in removing pollutants from surface waters. Researchers at the University of Kentucky (Barfield et al., 1978, 1979; Hayes, 1979; Hayes et al., 1982, 1984; Tollner et al., 1976, 1977) developed and tested a model (GRASSF) for filtration of suspended solids by artificial grass media. The model is based on the hydraulics of flow, and transport and deposition profiles of sediment in laboratory conditions. This physically based model takes into account a number of important field parameters that affect sediment transport and deposition through the filter (sediment type and concentration, vegetation type, slope and length of the filter). Flow is described by the continuity equation and steady state infiltration, i.e. flow decreases linearly from upstream to downstream in the filter.

Wilson et al., (1981) modified and incorporated GRASSF into SEDIMOT II, a hydrology and sedimentology watershed model. A simple algorithm to calculate the outflow hydrograph was incorporated into the model and up to three different slope changes throughout the filter could be considered. The model does not handle time dependent infiltration, an accurate description of flow through the filter, and changes in flow derived from sediment deposition during the storm event.

Several authors (Flanagan et al., 1989; Williams and Nicks, 1988; Nicks et al., 1991) have used the CREAMS model (Knisel, 1980) to evaluate the performance of VFS. However, as pointed out by Dillaha and Hayes (1991), CREAMS does not simulate the principal physical processes affecting transport in VFS and its applicability is questionable. The CREAMS simulations modify the erosion parameters of the downslope area to reflect increased roughness in the filter. However, the hydrology component does not take into account the changes in runoff volume or peak rates from the site caused by the filter.

The purpose of this work is to present and evaluate using experimental field data, a model (VFSMOD) to study hydrology and sediment transport through VFS. The model combines the strength of: a) a numerical submodel to describe overland flow and infiltration, b)

the University of Kentucky's algorithm developed specifically for the filtration of suspended solids by grass. This model formulation effectively handles complex sets of inputs similar to those found in natural events. The improvements of this combined model over the GRASSF or SEDIMOT II models are the inclusion of: (a) state of the art description of flow through the filter; (b) changes in flow derived from sediment deposition; (c) physically based time dependent soil water infiltration; (d) handling of complex storm pattern and intensity; and (e) varying surface conditions (slope and vegetation) along the filter.

2. Model development

Several processes must be described to simulate hydrology and sediment transport in filter strips. The problem can be divided into two major mechanisms: hydrology, and sediment transport and deposition. Hydrology in this context involves overland flow routing and soil water infiltration. Overland flow routing describes the water movement over the land surface by calculating flow rates at positions along the hill slope (Woolhiser, 1975). Sediment transport depicts the distribution of sediment concentrations along the hill slope at different time steps. These two mechanisms must be modeled concurrently as the solution to the sediment transport relies on flow values at different times and locations given by the hydrology part of the problem.

Two main submodels, one for each of the mechanisms, are linked together to produce a field-scale single storm model. The model routes the incoming hydrograph and sedimentograph from an adjacent field through a VFS and calculates the outflow, infiltration and sediment trapping efficiency for that event.

2.1. Hydrology submodel: overland flow and soil infiltration

The hydrology submodel presented by Muñoz-Carpena (1993) and Muñoz-Carpena et al., (1993a,b) consists of a Petrov–Galerkin quadratic finite element (FE) overland flow submodel based on the kinematic wave approximation (Lighthill and Whitham, 1955):

$$\frac{\partial h}{\partial t} + \frac{\partial q}{\partial x} = i_e(t) = r(t) - f(t), \tag{1}$$

$$q = \alpha h^m = \frac{\sqrt{S_0}}{n} h^{5/3}, \tag{2}$$

where x is flow direction axis (m), t is time scale (s), $h(x,t)$ is vertical flow depth (m), $q(x,t)$ is discharge per unit width (m²/s), $i_e(t)$ is rainfall excess (m/s), $r(t)$ is rainfall intensity (m/s), $f(t)$ is infiltration rate (m/s), S_0 is bed slope (m/m) at each node of the system, α and m are the coefficients for coupling uniform flow Eq. (2) (Manning's), n is Manning's roughness coefficient dependent on soil surface condition and vegetative cover at each node of the system. The initial and boundary conditions are:

$$h = 0; \qquad 0 \leq x \leq L; \qquad t = 0,$$
$$\tag{3}$$
$$h = h_0; \qquad x = 0; \qquad t > 0,$$

where h_0 can be 0, a constant or a time dependent function, such as the incoming hydrograph from the adjacent field.

The overland flow model was coupled, for each time step, with an infiltration submodel based on a modification of the Green–Ampt equation for unsteady rainfall (Chu, 1978; Mein and Larson, 1971, 1973; Skaggs and Khaleel, 1982; Muñoz-Carpena et al., 1993b):

$$f_p = K_s + \frac{K_s M S_{av}}{F_p}, \tag{4}$$

$$K_s(t - t_p + t_0) = F - M\,S_{av}\,ln\!\left(1 + \frac{F}{M\;\;S_{av}}\right), \tag{5}$$

where f_p is the instantaneous infiltration rate, or infiltration capacity, for ponded conditions (m/s), K_s is the saturated vertical hydraulic conductivity (m/s), $M = \theta_s - \theta_i$ is the initial soil-water deficit (m³/m³), S_{av} is the average suction across the wetting front (m), F_p is the cumulative infiltration after ponding (m), F is the cumulative infiltration for the event (m), t is the actual time (s), t_p the time to ponding, and t_0 is the shift of the time scale to correct for not having ponded conditions at the start of the event.

Rainfall excess, i_e in Eq. (1), is calculated for a given rainfall distribution for each node and time
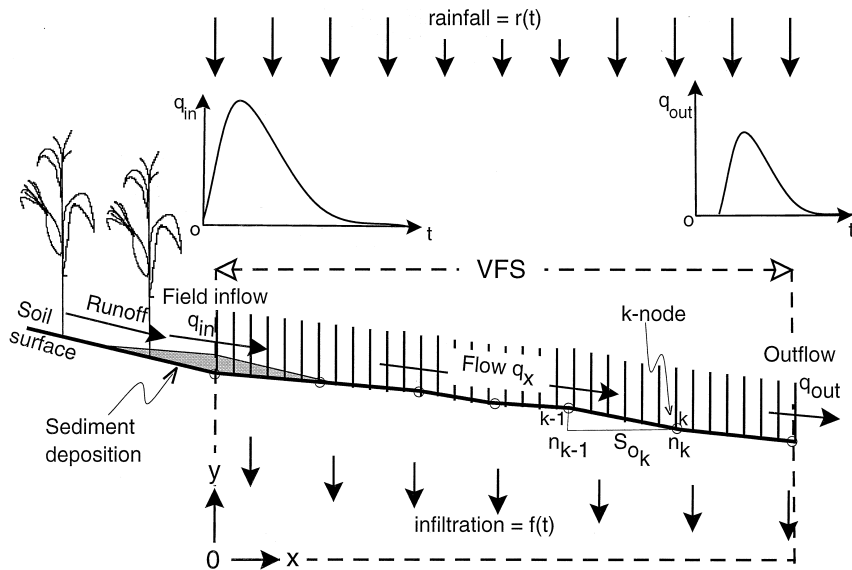
Fig. 1. Domain discretization for the FE overland flow submodel.

step by the infiltration model. The hydrograph representing runoff from the adjacent field is input as a time dependent boundary condition at the first node of the FE grid. The program allows for spatial variation of the parameters n and S_0 over the nodes of the system (Fig. 1). This feature of the program ensures a good representation of the field conditions for different rainfall events. The model can be operated to provide information on the effect of soil type (infiltration), slope, surface roughness, filter length, storm pattern and field inflow on VFS performance (i.e. reduction of

the runoff peak, volume and velocity) (Muñoz-Carpena et al., 1993b). It also describes the flow rate (q), velocity (V), and depth (h) components throughout the filter for each time step.

The numerical solution is subject to kinematic shocks, or oscillations in the solution that develop when a sudden change in conditions (slope, roughness or inflow) occurs. When linking the kinematic wave and the sediment transport models, the soil surface conditions are also changed for each time step, further increasing the potential for the kinematic shock
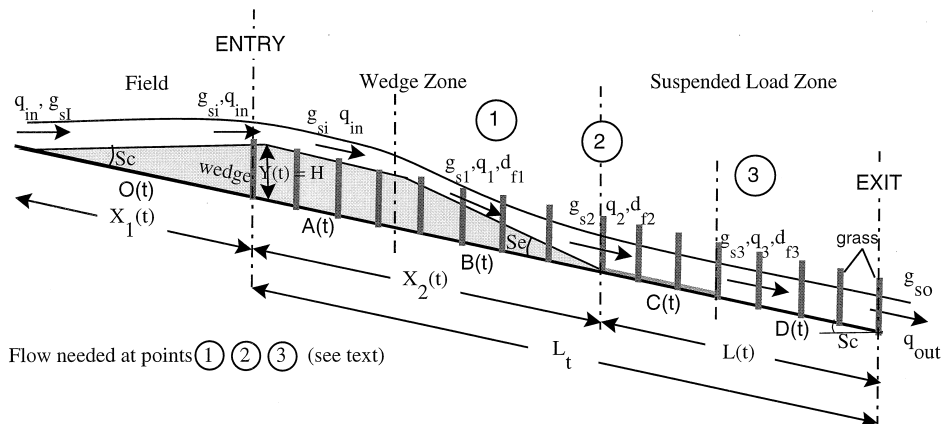
Fig. 2. Filter description for the sediment transport algorithm.

problem. VFSMOD implements a Petrov–Galerkin formulation (non-standard) FE to solve Eqs. (1) and (2). This solution procedure reduces the amplitude and frequency of oscillations with respect to the standard Bubnov–Galerkin method (Muñoz-Carpena et al., 1993a), thus improving the model stability and the sediment transport predictions which depend on overland flow values.

2.2. Sediment transport submodel

The University of Kentucky algorithm considers that during a rainfall/runoff event, field runoff reaches the upstream edge of the filter with time dependent flow rate q_{in} (cm^2/s), and sediment load g_{si} (g/cm/s). The vegetation produces a sudden increase in hydraulic resistance that slows the flow, lowers its transport capacity g_{sd} (g/cm-s), and produces deposition of the coarse material (particle diameter dp $>$ 0.0037 cm) carried mostly as bed load transport. The sediment trapped in this first part of the filter forms a geometrical shape that varies depending on the thickness of the deposited sediment layer at the entry of the filter, $Y(t)$ (m), and the effective top of vegetation, H (cm). A triangular shape at the adjacent field area and the beginning of the filter is formed when $Y(t) < H$. After $Y(t) = H$, a trapezoidal wedge is formed (Fig. 2) with three well defined zones: the upslope face of the wedge (with zero slope), $O(t)$ (cm); the upper face of the wedge (parallel to the soil surface), $A(t)$; and the downslope face, $B(t)$, with an equilibrium deposition slope Se for each time step (Fig. 2). Together these first filter zones are termed ''wedge zone'', and its length changes with time as sediment is deposited.

Zone $O(t)$, external to the filter, is important in explaining field observations where a portion of the sediment is deposited in the field area adjacent to the filter. After the wedge has formed, no sediment is deposited in zone $A(t)$ and the initial load, g_{si}, moves through to the next zone, $B(t)$. In this zone, deposition occurs uniformly with distance to the deposition edge, with transport mostly as bed load. The model assumes that the sediment inflow load, g_{si}, is greater than the downstream sediment transport capacity g_{sd} at point 2 (Fig. 2). The algorithm calculates the g_{sd} value for each time step and compares it with the sediment inflow load. If $g_{sd} > g_{si}$, all sediment is transported through the first part of the filter

(wedge), $g_{s2} = g_{sd}$, and the sediment is filtered at the suspended sediment zone (lower part of the filter). If $g_{sd} < g_{si}$ deposition at the wedge occurs and the fraction not deposited is filtered at the lower part of the filter, $g_{s2} = g_{in} - g_{sd}$. The calculation procedure utilizes a modified Manning's open channel flow equation, equation of continuity and Einstein's total transport function. Flow values at the filter entry and points 1 and 2 in Fig. 2 (q_{in}, q_1, q_2 respectively) are needed for these calculations.

After the downside of the wedge, two zones $C(t)$ and $D(t)$ form the ''suspended load zone'' or ''effective filter length'', $L(t)$ (Fig. 2). On zone $C(t)$, sediment has covered the indentations of the surface so that bed load transport and deposition occurs but the soil slope, S_c, is not significantly changed. All bed load transported sediment is captured before reaching zone $D(t)$, so only suspended sediment is transported and deposited in this zone until the flow reaches the end of the filter with sediment load g_{so}. The sediment trapping algorithm for the suspended load zone follows Tollner et al., (1976) equation based on a probabilistic approach to turbulent diffusion for non-submerged flow. Flow values at point three and filter exit, q_3 and q_{out} respectively (Fig. 2), are needed for these calculations. Details of the implementation of the submodel are given in Muñoz-Carpena (1993).

Mixed particle distribution is not included in the model formulation. The sediment filtration algorithm coded is that of the original work from Barfield et al., (1978, 1979) and Tollner et al., (1976, 1977). To account for real mixed particle sediment, a more simplified approach is taken similar to that used in the USDA-ARS KINEROS model (Woolhiser, 1990). In this model the median sediment particle diameter (d_{50}), read from the sediment particle distribution graph, represents an effective mean value for the plot and is used in the sediment filtration algorithm to predict sediment deposition. Ranges for sediment particle diameters for various soil textures can be estimated from work presented by Woolhiser et al., (1990).

2.3. Linkage between submodels

Flow conditions at the entry, exit and three inner points (1, 2, and 3) of the filter are needed for the sediment transport calculations (q_{in}, q_1, q_2, q_3 and
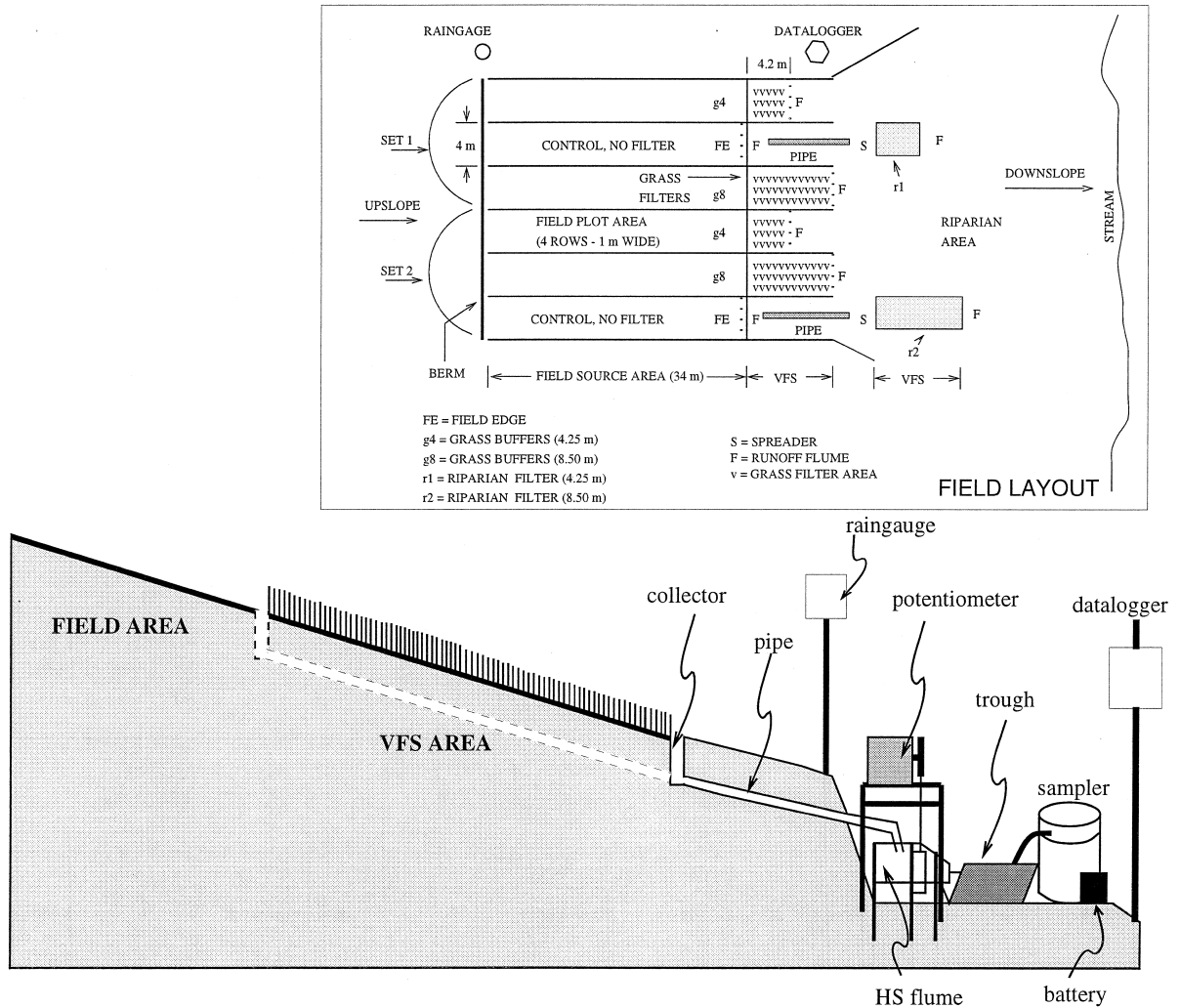
Fig. 3. Field layout and instrumentation at the experimental site.

q_{out} in Fig. 2). The GRASSF and SEDIMOT II models use a simple approach to calculating those values and do not consider the complex effects of rainfall, infiltration, and flow delay caused by the filter. A more accurate description of the flow conditions is obtained from the hydrology submodel presented before. In turn, the sediment transport model supplies information on changes in surface conditions (topography, roughness) due to sediment deposition during the event that affect overland flow.

During the simulation, feedback between the hydrology and sediment models is produced. The

hydrology model supplies the flow conditions at the five locations (entry, 1, 2, 3, and exit) set in the last time step (Fig. 2). The other parameters that interact through the linkage are the length, slope, and roughness in each of the sections (entry, 1, 2, 3, and exit).

After solving the sediment transport problem for a time step, new values of roughness and/or slope are selected as nodal values for the FE grid in zones $A(t)$ and $B(t)$, whereas $C(t)$ and $D(t)$ remain unchanged (Fig. 2). Changes in surface saturated hydraulic conductivity values (K_s) are considered negligible. The new surface parameters are fed back into the

hydrology model for the next time step. Surface changes are accounted for in this way.

The time step for the simulation is selected by the kinematic wave model to satisfy convergence and computational criteria of the FE method based on model inputs (Muñoz-Carpena et al., 1993a,b).

The incoming sedimentograph, g_{si} (g/s) during the simulation is obtained by multiplying the average sediment concentration for the event, C_i (g/cm^3) by the inflow rate, q_{in} (m^3/s), The implicit assumption is that water inflow is the major factor controlling the dynamic sediment inflow, more so that the varying sediment concentration throughout the storm. This assumption was tested by comparing curve shapes and mass of the incoming field sedimentographs with the reconstructed sedimentographs ($C_i * q_{in}$) for the simulated events and found to be acceptable. The proposed method improves the usability of the model as the C_i can be calculated from composite samples for the storm which are simpler to obtain from existing erosion plot experiments.

At the end of the simulation, the model outputs include: information on the water balance (volume of rainfall, field inflow, filter outflow and infiltration), hydrograph, sediment balance (field inflow, filter outflow and deposition), sedimentograph, filter trapping efficiency, and sediment deposition pattern within the filter (Muñoz-Carpena and Parsons, 1997).

3. Model testing

A field experimental site was set up for the purpose of calibrating and testing the model. Model inputs were measured or estimated from filter conditions and rainfall/runoff data collected for two years. One subset of the recorded events was used for calibrating the model and another for testing.

3.1. Experimental field setup

A field site in the North Carolina Piedmont region was selected to monitor the performance of VFS and riparian areas (Parsons et al., 1991). The soil at the site is a Cecil clayey, kaolinite, thermic, Typic Hapludult with a silty-loam surficial horizon (Parsons et al.,

1994). Six runoff plots with 4 m wide by 37 m long cropland source areas were constructed at the field. The slopes on the plots varied from 5% to 7%. Field rows were parallel to the slope to maximize runoff and erosion and enable testing of the filters under the worst conditions.

Surface runoff was collected at the field edge for two of the runoff plots (Fig. 3). Runoff from these control plots (no filter) was assumed to equal that of the adjacent field plots with filters. Two other plots had grass filter strips 4.3 m long and the remaining two had 8.5 m long strips. For these buffers, the ratio of the area of the field to the filter was 9 : 1 and 4.5 : 1, respectively. The grass stand was a mixture of fescue, bluegrass and bermuda grass. Two riparian filter plots were located further down slope. These areas were steep (18%–20% slope) with a vegetation mixture of trees and bushes. The surface runoff from the two non-filter plots was distributed at the upper edge of the two riparian plots. The riparian plots were 1.3 m wide with lengths of 4.3 and 8.5 m (area ratios of 27 : 1 and 13.5 : 1).

The quantity of runoff from each of the eight sampling points was measured with HS type flumes (0.15 m depth) (Brakensiek et al., 1979). The runoff from each plot was collected by a rain gutter and then piped to the flumes (Fig. 3). Water levels in the HS flumes were monitored with a potentiometer – float assembly. A half bridge with a 2 V excitation was used with the potentiometers providing voltage levels to measure water elevations in the flumes.

A portable datalogger (Campbell Scientific-CR10) was used at the site to monitor rainfall and surface runoff, and activate the water quality samplers. A tipping bucket rain gauge measures rainfall intensities and volumes at 5 min intervals (Fig. 3). The datalogger monitors and records the flume water levels during storm events every 30 s. Discrete automatic water quality samplers were installed on each of the eight plots. The samplers contain 24 one-liter bottles. The water quality sampler took a sample whenever the flume water level increased or decreased by 5 mm or more. The inlets for the samplers were located in a plywood trough downstream of the flume. Collected samples were analyzed for sediment concentrations and particle size distributions (Gee and Bauder, 1986).

Table 1
Field parameters governing the model

	Symbol	Description	Values	Units
General	N	Number of modes	27–50	–
	CR	Courant's number	0.8	–
	TTIME	Total simulation time	1800–3900	s
Hydrology component	L	Filter length	4.25–8.50	m
	W	Filter width	1.27–3.87	m
	S_{ok}	Slope at each node (k = 1,N)	0.02–0.20	–
	n_k	Manning's n (k = 1, N)	0.10–0.45	$s/m^{1/3}$
	K_s	Saturated hydraulic conductivity	2.5×10^{-6}–3.5×10^{-5}	m/s
	θ_s	Saturated water content	grass filters: 0.311	m^3/m^3
			riparian filters: 0.306	
	θ_i	Initial water content	0.100–0.310	m^3/m^3
	S_{av}	Sunction at the wetting front	grass filters: 0.379	m
			riparian filters: 0.088	
Sediment Component	n_m	Modified grass Manning's n	0.012	$s/cm^{1/3}$
	n_b	Manning's n for bare soil	0.04	$s/m^{1/3}$
	d_p	Median particle size, d_{50}, of incoming sediment	0.0003–0.0029	cm
	γ_s	Sediment weight density	2.60–2.65	g/cm^3
	V_f	Fall velocity of sediment	0.0004–0.0760	cm/s
	S_s	Media spacing	grass filters: 2.2	cm
			riparian filters: 10.0	
	H	Media height	15	cm
	P	Porosity of deposited sediment	0.434	–
	C_I	Inflow concentration	0.00075–0.03402	g/cm^3
	COARSE	proportion of fine sediment	100	%

3.2. Input parameters for the model

3.2.1. Model inputs for the hydrology submodel

The input parameters for the hydrology part of the model (overland flow + infiltration) are summarized in Table 1. More details on the selection of these parameters can be found in Muñoz-Carpena (1993) and Muñoz-Carpena and Parsons, (1997). Different procedures were used to identify these parameters for field testing the model.

The filter length and width were measured directly in the field. Nodal slopes were determined by a topographical field survey. A dense grid was laid down on the areas (a total of 191 points: 24 points in each of the short strips, 45 in each long strip). The transversal values of slope (to the direction of flow) were averaged to obtain a width-averaged set of slopes for each strip. These values were used for simulation purposes. A 1-D grid of 50 nodes was selected for each strip with 7–14 segments of equal slope. The range of slopes can be found in Table 1.

Manning's roughness coefficients were estimated from the literature values to match field conditions (Woolhiser, 1975; Engman, 1986; Woolhiser et al., 1990; Arcement and Schneider, 1989). These values change seasonally as a function of the vegetative conditions of the cover (higher values in summer, lower values in winter). Based on the references, the range considered in the field testing was 0.10–0.60 for grass buffers and 0.10–0.45 for riparian vegetation.

The saturated water content (θ_s) was measured in the laboratory from undisturbed soil cores, and suction at the soil wetting front (S_{av}) was determined from soil suction curves obtained from the soil cores from each filter area (Klute, 1986). Saturated vertical hydraulic conductivity values at the surface, K_s, were also measured from soil cores in the laboratory (Klute and Dirksen, 1986). Infiltrometer tests were conducted in the field (Bower, 1986). These values were highly variable ranging from 2.78×10^{-7} to 1.33×10^{-5} m/s.
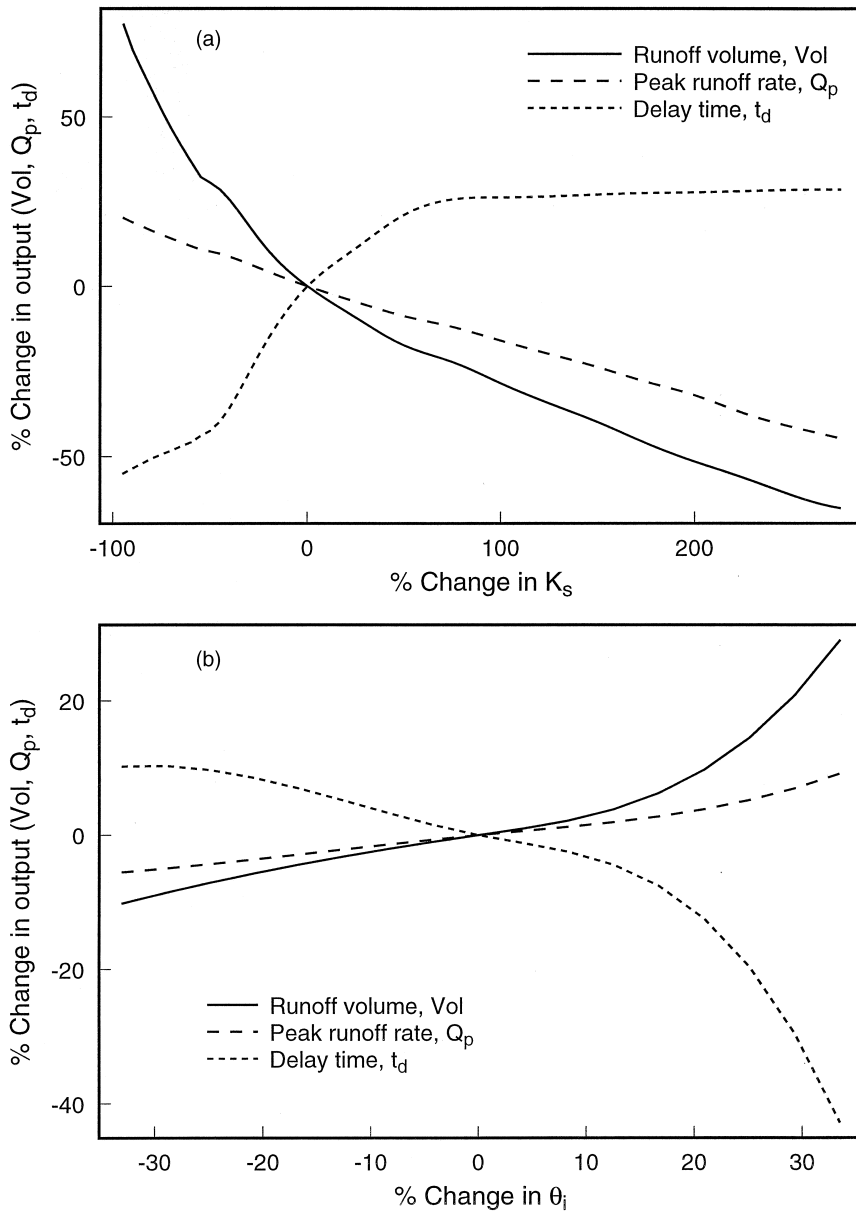
Fig. 4. (a-b) Sensitivity of model hydrological outputs to saturated hydraulic conductivity (a) and soil initial moisture content (b) values.

3.2.2. Model inputs for the sediment submodel

The field parameters that describe the sediment filtration process in this model are summarized in Table 1. The modified n_m and grass spacing, S_s, values were selected from the type of vegetation in the grass filters (Hayes et al., 1982). For a fescue/bluegrass/ bermuda grass mixture found at the experimental site, a value of $n = 0.012$ s/cm$^{1/3}$ and $S_s = 2.2$ cm is recommended. The spacing value matches vegetation counts measured at the experimental site (Muñoz-Carpena, 1993). For the riparian area, $S_s = 10.0$ cm was selected by field inspection.
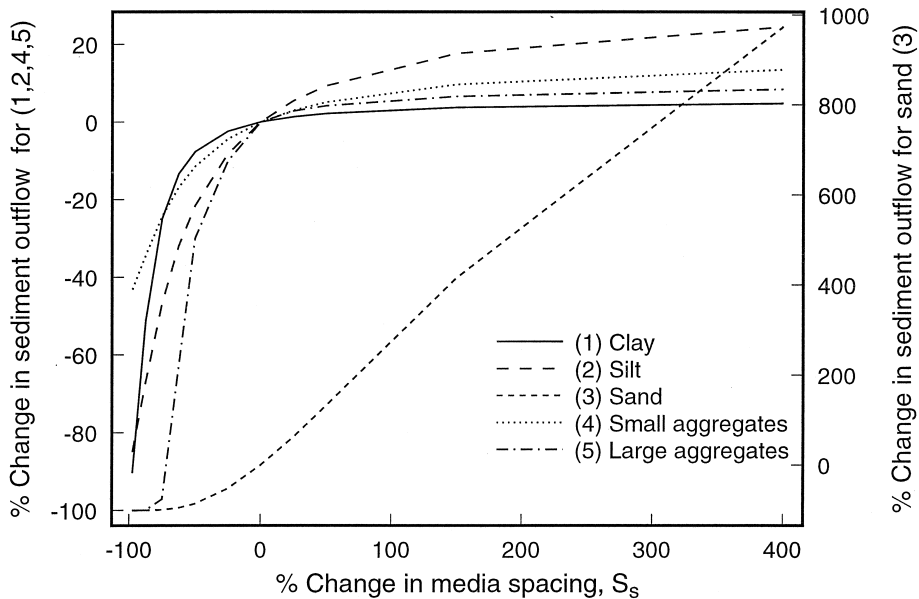
Fig. 5. Sensitivity of model sediment outputs to media spacing and sediment class

The parameter H was selected as 15 cm for our field situation, where the grass was maintained erect at least at that height. The porosity of the deposited sediment, P, was selected as 0.434 (Hayes, 1979).

Ranges for sediment particle size (d_{50}), fall velocity and density were chosen from soil texture based on tabulated data (Woolhiser et al., 1990). Soil texture of the surficial soil horizon was measured from a total of 15 samples taken at different surface points in the agricultural field source area (upper, medium and lower sections), and the filter areas. For the surficial silty-loam at the experimental site, a range of median particle sizes (d_{50}) from 0.0003 to 0.005 cm, was selected. The actual value for each event depends not only on soil texture but also on flow conditions (energy of the overland flow). As fall velocity is related to particle size, the term *particle class* will be used to denote these two characteristics plus sediment density.

The average sediment inflow concentration for the model, C_i (g/cm^3), was obtained from field data for each event by dividing the total sediment, coming from the agricultural source area into the filters, by the total volume of water inflow giving a range from 0.00075 to 0.03402 g/cm^3 (Table 1).

3.3. Analysis of sensitivity of the model to the input parameters

A sensitivity analysis was performed to gain some insight in the dependence of model outputs on certain model parameters and to assist in the model calibration. Some initial testing showed that the main parameters controlling the hydrology outputs were K_s and θ_i whereas the model was fairly insensitive to changes in θ_s and S_{av} values. Previous research (Muñoz-Carpena et al., 1993a) showed that Manning's n controls mainly the time to peak of the outgoing hydrograph.

A detailed sensitivity analysis was conducted for the parameters K_s, θ_i and Manning's n. Starting with measured values ($K_{sl} = 1.33 \times 10^{-5}$ m/s, $\theta_s = 0.311$ cm^3/cm^3), three sets of 115 simulations each were carried out for a range of ($0.05\,K_{sl} < K_s < 4\,K_{sl}$) (23 steps), and ($0.5\,\theta_s < \theta_i < \theta_s$) (5 steps). For each set, a different n was selected ($n = 0.1$–0.5). In these simulations, field measured values for θ_s and S_{av} were used (Table 1) and the additional inputs (filter characteristics, rainfall distribution and field inflow) were taken from an event recorded at the experimental site on 06/30/91 for a grass strip 4.3 m long.
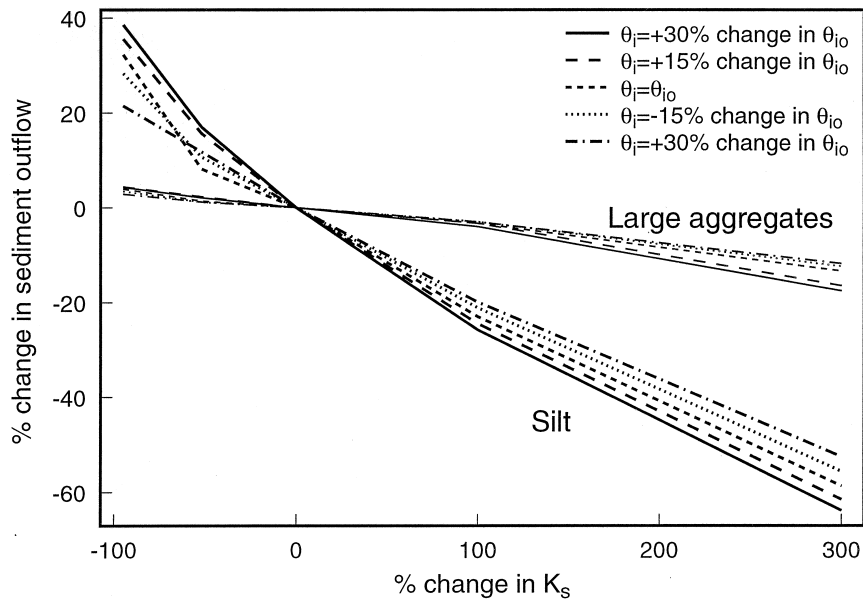
Fig. 6. Interaction between sensitive hydrological parameters and sediment outflow for some sediment classes.

Several quantities for the output hydrographs were obtained and compared for each simulation: delay time (t_d), time to peak (t_p), peak flow rate (Q_p), and total runoff volume (Vol). The results of the sensitivity analysis show that the output values Vol, t_d, and Q_p are sensitive to the parameters K_s and θ_i. Fig. 4(a) shows how a 100% increase in K_s translates into a 100% decrease in Vol and Q_p, and a 100% increase in t_d. Fig. 4(b) shows how a 60% increase in θ_i led to a 20% and 40% increase in Vol and Q_p, respectively, and a 50% decrease in t_d. The t_p was not significantly affected by the changes in K_s or θ_i (not shown). An interaction between K_s and θ_i was observed for low values of K_s. This is explained by the fact that for lower values of K_s the delay time is controlled by the soil moisture deficit (higher deficit, greater delay), but for higher K_s values, infiltration is sufficient to absorb the instantaneous rainfall intensity and the field inflow, regardless of the initial moisture deficit.

Initial testing on the sediment component of the model showed that the main parameters controlling sediment outflow are media spacing, S_s, and particle class. Variations in the modified Manning's n_m had relatively little effect on the output and the media height, H, was only visible for large events after the

trapezoidal wedge was formed at the filter. A detailed analysis was performed by varying grass spacing ($0.05 < S_s < 10$ cm) and particle classes (clay, silt, sand, small aggregates and large aggregates) (USDA Soil Survey Staff, 1975; Muñoz-Carpena, 1993). The remaining model inputs were obtained from the same field event as described before, and setting $K_s = K_{sl}$, $\theta_I = 0.20$, $n_m = 0.012$ cm/s$^{1/3}$, and $H = 15$ cm.

Fig. 5 shows the sediment outflow to be sensitive to particle class and grass spacing. Increases in total sediment outflow predictions of 100%–120% took place for each of the USDA Soil Survey Staff (1975) particle classes when S_s was increased 500%. For finer sediment classes most of the reduction took place in the lower range of the grass spacing values ($0.05 < S_s < 10$ cm) and the outflow became insensitive to further increases in S_s, whereas for the coarser sediment (sand) the increase was uniform. The explanation lies in the fact that for finer sediment the filtration process is performed mostly from suspended sediment in the suspended load zone of the filter ($L(t)$ in Fig. 2), where S_s is the governing parameter, whereas for sand most of the filtration takes place as deposition in the sediment wedge which depends on bed load transport relations and not on S_s.

An additional batch of simulations was conducted

Table 2
Statistics used to assess quality of the model results

Description	Symbol	Equation	Auxiliary Equations	Best Fit
Pearson square moment	PSM	$\left(\dfrac{n\sum Y_{oi}Y_{pi} - (\sum Y_{oi})(\sum Y_{pi})}{\sqrt{n\sum Y_{oi}^2 - (\sum Y_{oi})^2}\sqrt{n\sum Y_{pi}^2 - (\sum Y_{pi})^2}}\right)^2$		1.0
Weighted Pearson moment	PWM	$\dfrac{A}{B}\dfrac{n\sum Y_{oi}Y_{pi} - (\sum Y_{oi})(\sum Y_{pi})}{\sqrt{n\sum Y_{oi}^2 - (\sum Y_{oi})^2}\sqrt{n\sum Y_{pi}^2 - (\sum Y_{pi})^2}}$	$A = \dfrac{1}{2}\dfrac{(\sum Y_{oi}^2 + \sum Y_{pi}^2)}{\sum Y_{oi}}$ $B = \dfrac{1}{2}\dfrac{(\sum Y_{oi}^2 + \sum Y_{pi}^2)}{\sum Y_{pi}}$	$\pm$ 1.0
Sample correlation coefficient for the 1:1 line	$R_{1:1}^2$	$1 - \dfrac{1/(n-2)\sum(Y_{oi}-Y_{pi})^2}{1/(n-1)\sum(Y_{oi}-\bar{Y}_{oi})^2}$		1.0
Root mean square error	RMSE	$\sqrt{\dfrac{1}{n}(\sum \mathrm{Res}_i^2 - \dfrac{1}{n}\sum(\mathrm{Res}_i)^2)}$	$\mathrm{Res}_i = (Y_{oi} - Y_{pi})$	0.0
Means square error	MSE	$\dfrac{1}{n-1}(\sum \mathrm{Res}_i^2 - \dfrac{1}{n}\sum(\mathrm{Res}_I)^2)$	$\mathrm{Res}_i = (Y_{oi} - Y_{pi})$	0.0

to test the interaction between hydrology sensitive inputs and sediment outputs. Initial values of saturated hydraulic conductivity and initial soil moisture content were chosen ($K_s = K_{sl}$, $\theta_i = \theta_{io} = 0.218$), then varied ($0.95K_{sl} \le K_s \le 2K_{sl}$; $0.70\theta_{io} \le \theta_i \le 1.3\theta_{io} = \theta_s$), and sediment output recorded for each simulation. This procedure was repeated for each of the five particle classes mentioned earlier. Fig. 6 depicts the results for two of the sediment classes (clay and large aggregates). The analysis yielded similar results for four sediment classes (clay, silt, small, aggregates and sand) where $a \pm 100\%$ change in the K_s value results in an average $\pm 25\%$ change in sediment outflow, with some variation around that average ($\pm 20\%$–38%) introduced by the θ_i value. The remaining particle class (large aggregates) showed to be less sensitive to changes in hydrology parameters, with only a 3.5% variation in sediment outflow obtained in the procedure (Fig. 6). This is because of the fact that large aggregates are quickly retained at the entrance of the filter and infiltration does not play a significant role in the trapping process.

3.4. Model testing procedure

The procedure was divided into two steps: an initial calibration using a subset of field data for each event and subsequent field testing using the remaining data for the event. The calibration and testing of the hydrology component was done first as the sediment component builds on these results. The parameters optimized in the calibration process were those for which the model was found to be most sensitive (K_s, θ_i, and d_{50}).

Two data subsets were prepared for each event where runoff data was collected from the two filter lengths, one subset for each filter length (4.25 and 8.5 m). Calibration of the hydrology component was performed by adjusting K_s and θ_i to match observed outflow data (Vol, t_d, t_p, Q_p) on one of the filter lengths. Testing was carried out for that event by running the model for the other filter length with the parameters from the calibration run (modifying only the length and slope on the filter) and comparing the results with the observed data for that filter.

After calibration of the hydrology submodel, the sediment submodel was calibrated following the same approach by adjusting sediment class (d_{50}) within the suggested range (0.0003–0.005 cm) to match total sediment outflow and minimize error between predicted and observed pollutographs. No hydrology inputs were modified during this process. There was insufficient field data to perform a complete field testing of the sediment component in the manner described earlier, though the response obtained during the calibration using parameter ranges consistent with physical characteristics at the site show the ability of the model to describe the field process.

Table 3
Field calibration and testing of the hydrology component

No.	Event	V	Rain S^a (mm)	n	K_s (m/s)	θ_I	Vol Pred. (m³)	Vol Obs. (m³)	Vol Error (%)	t_d Pred. (s)	t_d Obs. (s)	t_d Error (%)	t_p Pred. (s)	t_p Obs. (s)	t_p Error (%)	Q_p Pred. (m³/S)	Q_p Obs. (m³/S)	Q_p Error (%)
Field Calibration																		
1	183 – 91	g4	25.2	0.10	1.33×10^{-5}	0.200	1.0880	1.1210	− 2.9%	1186	812	46.1%	1653	1622	1.9%	2.06×10^{-3}	1.89×10^{-3}	9.0%
2	112 – 92	g4	11.9	0.40	1.33×10^{-5}	0.310	0.1674	0.1873	− 10.6%	619	695	− 11.0%	1122	1295	− 13.4%	3.88×10^{-4}	3.46×10^{-4}	12.1%
3	112 – 92	r1	11.9	0.45	2.10×10^{-5}	0.200	0.1394	0.1129	23.5%	893	815	9.5%	1071	1355	− 21.0%	2.99×10^{-4}	2.62×10^{-4}	14.1%
4	151 – 92	g4	3.0	0.40	5.00×10^{-6}	0.308	0.1874	0.1905	− 1.6%	803	545	47.4%	1610	1865	− 13.7%	1.62×10^{-4}	1.25×10^{-4}	30.4%
5	168 – 92	g4	4.6	0.40	5.00×10^{-6}	0.275	0.1069	0.1184	9.7%	417	455	8.4%	909	1025	11.3%	2.04×10^{-4}	1.66×10^{-4}	− 23.1%
6	178 – 92	g4	33.0	0.40	1.33×10^{-5}	0.100	1.6520	1.6120	− 2.5%	646	694	7.0%	915	935	2.2%	3.15×10^{-3}	2.50×10^{-3}	− 25.7%
7	178 – 92	r1	33.0	0.30	1.71×10^{-5}	0.100	1.9990	2.2980	13.0%	455	455	0.1%	863	935	7.7%	3.26×10^{-3}	3.70×10^{-3}	11.9%
8	309 – 92	g8	6.9	0.40	1.00×10^{-5}	0.311	0.2938	0.2896	− 1.5%	311	245	− 27.2%	747	665	− 12.4%	1.05×10^{-3}	5.06×10^{-4}	− 107.8%
9	309 – 92	r1	6.9	0.30	3.50×10^{-5}	0.100	0.1104	0.1120	1.4%	541	575	5.9%	603	635	5.0%	1.53×10^{-3}	1.54×10^{-4}	− 89.3%
10	309 – 92	r2	6.9	0.30	1.00×10^{-5}	0.306	0.5514	0.6246	11.7%	309	335	7.6%	619	1265	51.1%	1.86×10^{-3}	6.47×10^{-4}	− 188.1%
11	331a – 92	g4	13.0	0.40	1.33×10^{-5}	0.305	0.6482	0.6411	− 1.1%	317	395	19.8%	598	545	− 9.7%	2.28×10^{-3}	2.46×10^{-3}	7%
12	331a – 92	r2	13.0	0.30	1.71×10^{-5}	0.305	0.6687	0.7118	6.1%	303	395	23.2%	589	665	11.5%	1.80×10^{-3}	1.83×10^{-3}	2%
13	331c – 92	g8	9.4	0.40	2.50×10^{-6}	0.311	1.0860	1.0350	− 4.9%	306	365	16.1%	1245	1115	− 11.7%	1.30×10^{-3}	1.06×10^{-3}	− 22%
14	331c – 92	r2	9.4	0.30	3.00×10^{-6}	0.200	0.5606	0.5069	− 10.6%	788	365	− 116.0%	1162	1055	− 10.1%	8.87×10^{-4}	5.67×10^{-4}	− 56%
15	24 – 93	g4	7.1	0.40	1.33×10^{-5}	0.305	0.3240	0.3687	12.1%	309	395	21.7%	619	1175	47.3%	5.72×10^{-4}	5.68×10^{-4}	− 1%
16	24 – 93	r1	7.1	0.30	3.50×10^{-5}	0.200	0.2803	0.2717	-3.2%	519	605	14.2%	1192	1475	19.2%	4.48×10^{-4}	3.95×10^{-34}	-13%
Field Testing																		
17	183 – 91	g8	25.2	0.10^b	1.33×10^{-5}	0.200	0.4210	0.4429	− 4.9%	1686	1622	3.9%	1793	1802	− 0.5%	1.34×10^{-3}	9.68×10^{-4}	38.5%
18	112 – 92	g8	11.9	0.40	1.33×10^{-5}	0.308	0.0524	0.0550	− 4.7%	623	755	− 17.5%	1480	1625	− 8.9%	1.14×10^{-3}	8.55×10^{-5}	33.8%
19	112 – 92	r2	11.9	0.45	2.10×10^{-5}	0.200	0.0000	0.0000	0.0%	0	0	0.0%	0	0	0.0%	0.00×10	0.00×10	0.0%
20	151 – 92	g8	3.0	0.40	5.00×10^{-6}	0.308	0.0000	0.0000	0.0%	0	0	0.0%	0	0	0.0%	0.00×10	0.00×10	0.0%
21	168 – 92	G8	4.6	0.40	5.00×10^{-6}	0.300	0.0403	0.0469	14 – 1%	790	1055	25.1%	1128	1085	− 4.0%	1.30×10^{-3}	7.92×10^{-5}	− 64.1%
22	178 – 92	g8	33.0	0.40	1.33×10^{-5}	0.100	1.3630	1.4710	7.3%	648	425	− 52.6%	1027	965	− 6.4%	3.24×10^{-3}	2.52×10^{-3}	− 28.5%
23	178 – 92	r2	33.0	0.30	1.71×10^{-5}	0.100	1.8430	1.7900	− 3.0%	459	425	− 8.1%	891	905	1.5%	3.33×10^{-3}	2.52×10^{-3}	− 0.6%
24	331a – 92	g8	13.0	0.40	1.33×10^{-5}	0.305	0.4964	0.5240	5.3%	316	395	20.0%	720	725	0.8%	1.63×10^{-3}	1.44×10^{-3}	− 13%
25	331c – 92	g4	9.4	0.40	1.33×10^{-5}	0.305	0.7706	0.7396	− 4.2%	777	515	− 50.9%	1166	1115	− 4.6%	1.09×10^{-3}	9.01×10^{-3}	− 21%
26	24 – 93	g8	7.1	0.40	1.33×10^{-5}	0.305	0.1318	0.1608	18.0%	304	395	23.1%	1261	1475	14.5%	3.77×10^{-4}	2.82×10^{-4}	− 34%
27	24 – 93	r2	7.1	0.30	3.50×10^{-5}	0.200	0.0000	0.0000	0.0%	0	0	0.0%	0	0	0.0%	0.00×10	0.00×10	− 0.0%

[a] Filters as defined in Fig. 4
[b] Filters before grass development at the beginning of the experimental period
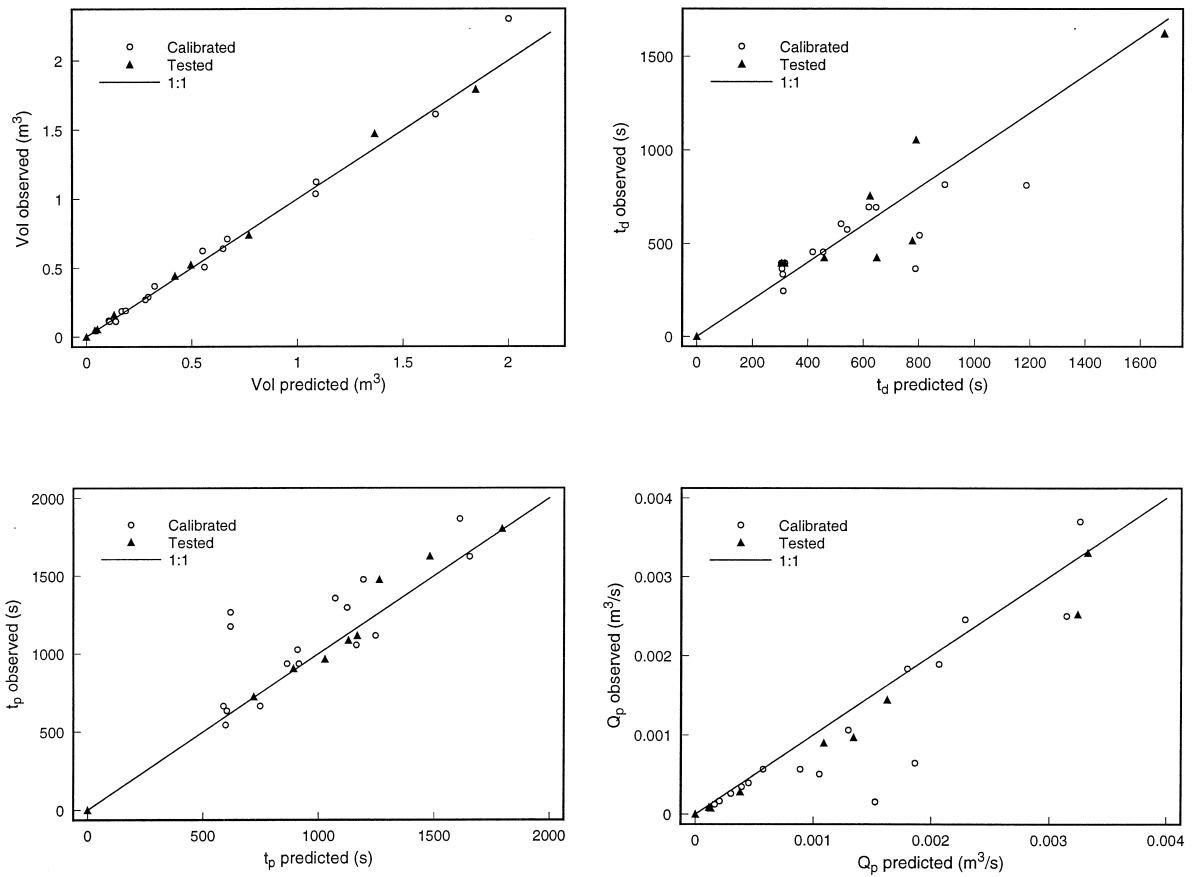
Fig. 7. (a–d) Comparison of observed versus predicted values for the hydrology component.

3.4.1. Statistical parameters used in the model testing process

Several types of statistics provide measures of the goodness of fit between simulated and observed values (James and Burgues, 1982; McCuen and Snyder, 1975). Table 2 summarizes five statistics that were used during model testing. A paired *t*-test

Table 4
Measures of goodness of fit of the hydrology component

	$R^2_{1:1}$	PSM[a]	PWM[a]	MSE[a]	RMSE[a]
Vol	0.99	0.92	0.92	4.55×10^{-3}	6.62×10^{-2}
T_d	0.76	0.75	0.79	25108	155.5
t_p	0.82	0.80	0.83	35357	184.5
Q_p	0.82	0.81	0.88	1.55×10^{-7}	3.86×10^{-4}

[a] As defined in Table 2

was also conducted to test if there was a significant difference in the means of predicted versus observed values (Ostle and Malone, 1988). The assumptions for the paired *t*-test were that both the simulated and observed data were from a normally distributed population and the null hypothesis was that the means from the two populations were equal.

3.4.2. Field calibration and testing of the hydrology component

A set of 27 events from the experimental site (1991–1993) was chosen to compare the predictions of the model with field values. Table 3 summarizes these results.

In the field calibration process initial values of $K_s = K_{sl}$, $n_k = 0.30$ and $\theta_i = 0.875$ θ_s (K_{sl} and θ_s are the measured values as described in Table 1) were chosen
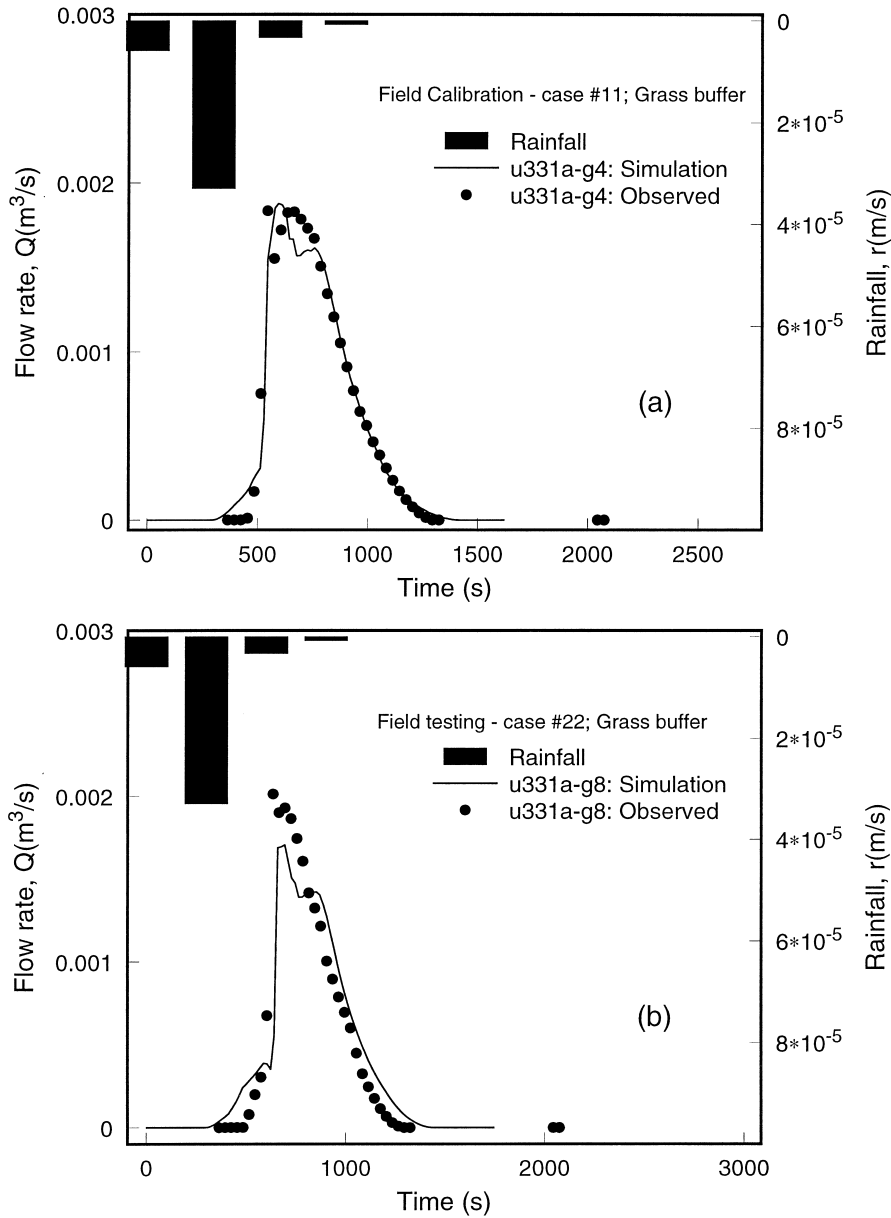
Fig. 8. (a–b) Example of results obtained during the field calibration (a, case #6 in Table 3) and testing (b, case #22 in Table 3) of the hydrology component.

and then varied within the range of ± 80% to fit the observed data (cases 1–16 in Table 3). The optimal values found in each case were used in the validation of hydrographs from other strips within the same date-event (cases 17–27 in Table 3). This approach assumes that K_s and n_b vary within the strips owing

to season and deposition of sediment from previous events.

The predicted set of results presented in Table 3 was compared with the observed values for the outputs: Vol, t_d, t_p, Q_p. These values are plotted against a 1 : 1 line (line of perfect agreement) in

Table 5
Field calibration of the sediment component

No.	Event	VFS[a]	Ss(cm)	Sediment Inflow			Sediment Outflow (g)		Error (%)	PWM	$R^2_{1:1}$
				d_{50} (cm)[b]	C^I (g/cm^3)[c]	Total sediment (g)	Predicted	Observed			
1	112 − 92	g4	2.2	0.0003	0.00108	287.0	30.5	30.9	1.3	0.92	0.87
2	112 − 92	r1	10.0	0.0006	0.00075	188.9	17.9	16.3	9.2	0.71	0.64
3	151b − 92	g4	2.2	0.0003	0.00244	968.3	20.1	20.0	0.72	0.71	0.64
4	178a − 92	g4	2.2	0.0029	0.03402	64759.5	2229.0	1738.3	− 28.2	0.91	0.84
5	178a − 92	g8	2.2	0.0029	0.03402	54884.2	4340.4	3989.2	− 8.8	0.75	0.55
6	178a − 92	r2	10.0	0.0029	0.03402	54884.2	12475.5	12862.1	3.0	0.78	0.73
7	331a − 92	g4	2.2	0.0008	0.00793	5788.0	2488.0	2497.1	0.4	0.74	0.66
8	331a − 92	g8	2.2	0.0004	0.00793	5788.0	345.0	429.2	19.5	0.73	0.51
9	024 − 93	g4	2.2	0.0003	0.01147	6187.8	639.0	662.5	− 3.5	0.78	0.62

[a] Filters as defined in Figure 4.
[b] Expected range for silty-loam soil surface; silt; $0.0003 < d_{50} < 0.005$ cm (Woolhiser et al., 1991).
[c] Measured for each storm.

Fig. 7(a–d). Good predictions were obtained in general though some outliers were found in the t_p and Q_p sets. Statistics obtained for all these quantities are summarized in Table 4. The best model predictions were obtained for the total outflow volume, Vol, and the worst for delay time, t_d. For each of the parameters, a paired t-test was done. Similar to the other statistics, the t-test results indicated that predictions of Vol and t_d were good while the means for predictions

of t_p and Q_p were statistically different from the observed means, probabilities greater than 0.95.

Fig. 8 shows the results for a calibration run on a grass filter of 4.25 m followed by the testing run on the grass filter of 8.50 m for the same event. The simulated hydrograph for the calibration run fit the observed values. The testing run on the 8.5 m grass filter underpredicted the peak although the shape was in good agreement with the observed hydrograph.
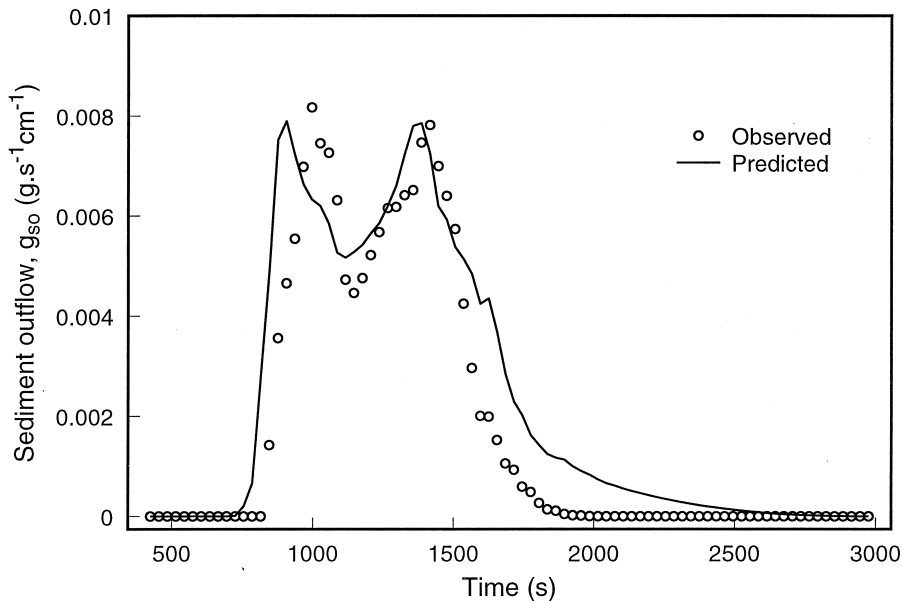
Fig. 9. Example of results obtained during the field calibration of the sediment component (case No.4 in Table 5).

Although the quality of the predictions was generally good, calibration or testing of the model was difficult in some cases especially where the calibration was poor (case 8, PWM = 0.47, $R^2_{1:1} = 0.27$). Non-laminar flow as a result of channelization of the flow during the season and other experimental artifacts may account for these results.

3.4.3. Field calibration of the sediment component

A subset of nine cases from the experimental site were chosen to compare sediment outflow predictions with field data (cases 2–4, 6–7, 11, 15 and 24 in Table 3). The input parameters used as a first approximation were those measured or derived from field conditions. The only adjustment needed in two of the nine cases was adjusting the d_{50} value within literature values for this kind of soil (Woolhiser et al., 1990). This confirms the idea that a correct handling of the filter hydrology, as the one provided in this study, is essential to obtain acceptable sediment outflow predictions when simulating natural (dynamic) events.

All predicted sediment graphs were compared with the observed data and the *PWM* and $R^2_{1:1}$ statistics calculated. Table 5 summarizes these results. Good predictions are obtained with the model in all but two cases. Comparisons of the average predicted sediment loss with the observed sediment loss with the paired *t*-test indicated that the means were statistically equal for probabilities of 0.66 or greater.

Fig. 9 shows an example from an event where the water runoff and sediment load from the field area was routed through a grass filter of $L = 4.3$ m (Case 4 in Table 5). The other parameters not included in Table 5 and used in all the simulations are as discussed in the model inputs section: modified Manning's $n_m = 0.012$ s/cm$^{1/3}$; media height, $H = 15$ cm; and porosity of deposited sediment, $p = 0.434$. The statistics calculated for this case were $R^2_{1:1} = 0.85$ and PWM = 0.91.

4. Conclusions

A single event, one-dimensional model, was developed and field tested. Field testing included selection and analysis of inputs, a sensitivity analysis of selected variables, and calibration and comparison of model results with field data.

The strength of this model compared with previous efforts lies in the better representation of field hydrology that leads to better sediment outflow predictions. The model applies a fundamental approach to the hydrology process by solving the physical equations (FE solution to the kinematic wave equation and Green–Ampt Infiltration approximation). This solution is linked (in time and space) with the University of Kentucky VFS model for sediment filtration through VFS.

The sensitivity analysis indicated that the most sensitive parameters were soil initial water content and vertical saturated hydraulic conductivity for the hydrology component of the model and particle class (particle size, fall velocity and sediment density), and grass spacing for the sediment component. Critical attention should be given in the selection of these parameters when running this model.

The model was tested for a North Carolina Piedmont experimental site. In general, good agreement was obtained between observed and predicted values. Some sources of variability were discussed. One such source was the complexity of the ''natural'' events. The handling of overland flow as sheet flow could pose problems when a filter is not properly maintained as suggested by some authors (Dillaha et al., 1986).

Field variability is an inherent source of error in any model validation, thus parameters to describe hydrology and sediment transport in VFS areas are highly variable. A range of variation in the saturated hydraulic conductivity parameters was needed to fit the model to observed data. This variation is explained by changes in surface conditions caused by seasonal and biological factors.

The nature of the mathematical formulation of the overland flow model and its numerical solution is also considered. Eulerian methods (FEs, finite differences) suffer from numerical oscillations when sudden changes in field conditions occur (kinematic shocks). The problem is minimized in this model formulation by the use of an improved numerical method (Petrov–Galerkin) (Muñoz-Carpena et al., 1993b).

References

Arcement, G.J., Schneider, V.R., 1989. Guide for selecting Manning's roughness coefficients for natural channels and flood plains. US Geological Survey, Water Supply Paper No. 2339.

Barfield, B.J., Tollner, E.W., Hayes, J.C.,1978. The use of grass filters for sediment control in strip mining drainage. Vol. I: Theoretical studies on artificial media. Pub. no. 35-RRR2-78. Institute for Mining and Minerals Research, University of Kentucky, Lexington.

Barfield, B.J., Tollner, E.W., Hayes, J.C., 1979. Filtration of sediment by simulated vegetation I. Steady-state flow with homogeneous sediment. Transactions of ASAE 22 (5), 540–545.

Bernard, O., Linda C. Malone, 1988. Statistics in Research, Iowa State University Press, Ames, Iowa, USA.

Bolton, S.M., Ward, T.J., Cole, R.A., 1991. Sediment-related transport of nutrients from southwestern watersheds. J. Irr. Drain. Eng. ASCE 117 (5), 736–747.

Bower, L.H., 1986. Intake Rate: Cylinder infiltrometer, Ch 3. In: Methods of Soil Analysis, 2nd. Ed. Part I. Physical and Mineralogical Properties. Am. Soc. Agron. Monograph 9:1. Madison, Wisconsin USA. pp 825–843.

Brakensiek, D.L., Osborn, H.B., Rawls, W.J., 1979. Field manual for research in agricultural hydrology, US Department of Agriculture, Agriculture Handbook 224. p. 50.

Cooper, J.R., Gilliam, J.W., Daniels, R.B., Robarge, W.P., 1987. Riparian areas as filters for agricultural sediment. Soil Soc. Am. Proc. 51, 416–420.

Chu, S.T., 1978. Infiltration during unsteady rain. Water Resour. Res. 14 (3), 461–466.

Daniels, R.B., Gilliam, J.W., 1989. Effect of grass and riparian filters on runoff and water quality. North Carolina. Soil Science Soc. Proc. 32, 37–45.

Dillaha, T.A., Sherrard, J.H., Lee, D., 1986. Long-term effectiveness and maintenance of vegetative filter strips. VPI-VWRRC-Bull. 153, Virginia Polytechnic Institute and State University, Blacksburg.

Dillaha, T.A., Reneau, R.B., Mostaghimi, S., Lee, D., 1989. Vegetative filter strips for agricultural nonpoint source pollution control. Transactions of ASAE 32 (2), 491–496.

Dillaha, T.A., Hayes, J.C., 1991. A procedure for the design of vegetative filter strips. Final Report to USDA Soil Conservation Service. Washington, DC, p. 48.

Engman, E.T., 1986. Roughness coefficients for routing surface runoff. J. Irrigation and Drainage Eng. ASCE 112 (1), 39–53.

Flanagan, D.C., Foster, G.R., Neibling, W.H., Hurt, J.P., 1989. Simplified equations for filter strip design. Transactions of ASAE 32 (6), 2001–2007.

Gee, G.W., Bouder, J.W., 1986. Particle size analysis, Ch. 15. In: Methods of Soil Analysis, 2nd. Ed., Part I. Physical and Mineralogical Properties, Am. Soc. Agron., Monograph 9:1. Madison, Wisconsin USA. pp. 383–409.

Hayes, J.C., 1979. Evaluation of design procedures for vegetal filtration of sediment from flowing water. unpublished Ph.D. dissertation, University of Kentucky, Lexington, KY, USA.

Hayes, J.C., Barfield, B.J., Barnhisel, R.I., 1982. The use of grass filters for sediment control in strip mine drainage. III. Empirical verification of procedures using real vegetation. Report No. IMMR82/070. Institute for Mining and Mineral Research, University. of Kentucky, Lexington, KY.

Hayes, J.C., Barfield, B.J., Barnhisel, R.I., 1984. Performance of grass filters under laboratory and field conditions. Transactions of ASAE 27 (5), 1321–1331.

James, L.D., Burgues, S.J., 1982. Selection, calibration and testing of hydrologic models, Ch. 11. In: Hydrologic Modeling of Small Watersheds, C.T. Haan, H.P. Johnson and D.L. Brakensiek Eds., ASAE Monograph no. 5, St. Joseph: ASAE, pp. 437–472.

Klute, A., 1986. Water retention: laboratory methods, Ch. 26: In: Methods of Soil Analysis, 2nd. Ed., Part I. Physical and Mineralogical Properties, Am. Soc. Agron. Monograph 9:1, Madison, Wisconsin USA. pp. 635–662.

Klute, A., Dirksen, C., 1986. Hydraulic conductivity and difussivity: laboratory methods, Ch. 28. In: Methods of Soil Analysis, 2nd. Ed., Part I. Physical and Mineralogical Properties, Am. Soc. Agron. Monograph 9:1, Madison, Wisconsin USA, pp. 687–734.

Knisel, W.G., 1980. CREAMS: A field-scale model for chemicals, runoff and erosion from agricultural management systems, US Department of Agriculture, Science and Education Administration, Conservation Report No. 26. Washington, DC, p. 643.

Lighthill, M.J., Whitham, C.B., 1955. On kinematic waves: flood movement in long rivers. Proc. R. Soc. London Ser. A 22, 281–316.

Lowrance, R.R., Sharpe, J.K., Sheridan, J.M., 1986. Long-term sediment deposition in the riparian zone of a Coastal Plain Watershed. J. Soil and Water Cons. 41, 266–271.

McCuen, R.H., Snyder, W.M., 1975. A proposed index for comparing hydrographs. Water. Resour. Res. 11 (6), 1021–1024.

Magette, W.L., Brinsfield, R.B., Palmer, R.E., Wood, J.D., 1989. Nutrient and sediment removal by vegetated filter strips. Transactions of ASAE 32 (2), 663–667.

Mein, R.G., Larson, C.L., 1971. Modelling the infiltration component of the rainfall-runoff process, Bulletin 43, University of Minnesota, MN, Water Resources Research Center.

Mein, R.G., Larson, C.L., 1983. Modeling infiltration during a steady rain. Water Resourc. Res. 9 (2), 384–394.

Mitsch, W.J., Gosselink, J.G., 1986. Wetlands. van Reinhold, New York, USA.

Muñoz-Carpena, R., 1993. Modeling hydrology and sediment transport in vegetative filter strips. unpublished Ph.D. dissertation. North Carolina State University, Raleigh.

Muñoz-Carpena, R., Miller, C.T., Parsons, J.E., 1993. A quadratic Petrov-Galerkin solution for kinematic wave overland flow. Water Resour. Res. 29 (8), 2615–2627.

Muñoz-Carpena, R, Parsons, J.E., Gilliam, J.W., 1993. Numerical approach to the overland flow problem in vegetative filter strips. Transactions of ASAE 36 (3), 761–770.

Muñoz-Carpena, R., Parsons, J.E., 1997. VFSMOD, Vol. 1, User's Manual, NC State University, Raleigh, NC.

Nicks, A.D., Williams, R.D., Krider. J.N., Lewis, J.A., 1991. Simulation of filter strip effectiveness. In: Proc. of the Environmentally Sound Agriculture Conference, A.B. Bottcher, K.L. Campbell, W.D. Graham, Eds., Orlando, FL, pp. 16–18.

Parsons, J.E., Daniels, R.B., Gilliam, J.W., Dillaha, T.A., 1991. The effect of vegetation filter strips on sediment and nutrient removal from agricultural runoff, In: Proc. of the Environmentally Sound Agriculture Conference, A.B. Bottcher, K.L. Campbell, W.D. Graham, Eds., Orlando, FL, pp. 16–18.

Parsons, J.E., Daniels, R.B., Gilliam, J.W., Dillaha, T.A., 1994. Reduction in sediment and chemical load in agricultural field runoff by vegetative filter strips, UNC-WRR Report no. 286, Water Resources Research Institute of the University of North Carolina, Raleigh, NC.

Skaggs, R.W., Khahee, R., 1982. Infiltration, Ch. 4, In: Hydrologic modeling of small watersheds. C.T. Haan, H.P. Johnson, D.L. Brakensiek, Eds., St. Joseph, MI, ASAE. pp. 121–168.

Tollner, E.W., Barfield, B.J., Haan, C.T., Kao, T.Y., 1976. Suspended sediment filtration capacity of simulated vegetation. Transactions of ASAE 19 (4), 678–682.

Tollner, E.W., Barfield, B.J., Vachirakornwatana, C., Haan, C.T., 1977. Sediment deposition patterns in simulated grass filters Transactions of ASAE 20 (5), 940–944.

USDA Soil Survey Staff. 1975. Soil Taxonomy: A Basic System of Soil Classification for Making and Interpreting Soil Surveys. USDA-SCS. Agricultural Handbook, 436. US Government Printing Office, Washington, DC.

Williams, R.D., Nicks, A.D., 1988. Using CREAMS to simulate filter strip effectiveness in erosion control. J. of Soil and Water Conservation 43, 108–112.

Wilson, L.G., 1988. Sediment removal from flood water by grass filtration. Transactions of ASAE 10 (1), 35–37.

Wilson, B.N., Barfield, B.J., Moore, I.D., 1981. A hydrology and sedimentology watershed model, Part I, Modeling Techniques. Technical Report. Department of Agricultural Engineering. University of Kentucky. Lexington.

Woolhiser, D.A., 1975. Simulation of unsteady overland flow, In: Unsteady Flow in Open Channels, Vol. II, K. Mahmood, V. Yevjevich, Eds., Fort Collins: Water Resources.

Woolhiser, D.A., Smith, R.E., Goodrich, D.C., 1990. KINEROS, A Kinematic Runoff and Erosion Model: Documentation and User Manual, USDA-ARS, ARS-Publication no. 77.

Young, R.A., Huntrods, R., Anderson, W., 1980. Effectiveness of vegetative buffer strips in controlling pollution from feedlot runoff. J. Environ. Qual. 9, 483–487.